Contrib. Astron. Obs. Skalnaté Pleso **38**, 479 – 500, (2008)

Optical behavior of cosmic dust particles with volatile icy coating

M. Kocifaj

Astronomical Institute of the Slovak Academy of Sciences, Interplanetary Matter Division, Dúbravská cesta 9, 845 04 Bratislava, The Slovak Republic, (E-mail: kocifaj@savba.sk)

Received: January 21, 2008; Accepted: April 15, 2008

Abstract. The scattering properties of composite evaporating interplanetary dust particles are analyzed. A two-component particle (usually supplying e.g. cometary dust) is considered in the form of a solid inclusion surrounded by a volatile ice shell. The processes of evaporation lead to a continuous decrease of the particle size because of ice loss, implying evolution of the optical properties of such particle. If a realistic model of the Gaussian core with ice coating is replaced by a volume equivalent homogeneous sphere, the numerical simulations become much easier and straightforward. But, the accuracy of calculation results is questionable because of hard limitations originated from Mie theory (which is strictly applicable to homogeneous spherical targets). Our results show that the Gaussian particle is a less efficient scatterer compared with the volume equivalent homogeneous sphere, especially when the particle's size is close to or larger than the wavelength of an incident radiation. The polarization features of the Gaussian particle differ from those of a homogeneous sphere. This can be an important fact in distiguishing between these two particle models. Substitution of realistically shaped and composite particles by idealized homogeneous spheres may definitely lead to a misinterpretation of measured optical data as well as to retrieval of incorrect microphysical characteristics of dust particles.

Key words: composite dust particles – polarization and scattering features – Gaussian core – ice coating

1. Introduction

Dust particles moving in the Solar system undergo a plentitude of physical and/or chemical variations due to a set of interactions (Moro-Martìn and Malhotra, 2003). For instance, a dust particle may collide with other ones (Steel and Elford, 1986) and, if not destroyed, it can jump to another trajectory. Concurrently, the effects of electromagnetic radiation (Klačka 2004), Lorentz force (Holmes et al., 2003) or sputtering (Le Sergeant D'Hendecourt and Lamy 1981) can dramatically change the orbital evolution of such particle. In principle, the sputtering is responsible for erosion of dust particles (Kapišinský 1984) and thus for a continuous reduction of the particle's size. A rapid mass loss occurs if a particle consisting of valatile materials is approaching the Sun. As a consequence

the particle's surface is subject to abrupt chemical alteration, especially when vaporable elements are preferrably distributed in the shell of the particle. Efficiency of the particle shrinking depends not only on how far away from the Sun a particle is situated, but also on its chemistry (Mukai, 1973).

The size and shape fluctuations, and chemical processes on dust grains are experimentaly indicated by evolving optical properties of interplanetary dust particles while they spiral toward the Sun (Levasseur-Regourd, 2003). For instance, the linear polarization P at 90-100 degrees becomes an evident function of solar distance (Dumont and Levasseur-Regourd, 1988), and this functional behavior is related to evaporation and sputtering effects. To simulate the evaporation processes it is necessary to find the equilibrium temperature of a grain by solving an equation of the energy balance (Posch et al, 2002). Lamy (1974) has already pointed out that interplanetary grains experience a large temperature variation in the Solar system. It is therefore not unusual that the mass loss will significantly vary with the heat capacity of individual constituents of a dust grain (Davidsson and Gutiérrez, 2006; Handa and Klug, 1988).

In general, interplanetary dust particles are complex aggregates having different origin and thus non-equal composition (Flynn, 1994). Nevertheless, the minor elements are usually omitted and only dominant constituents are considered in common dust modeling. Typically cometary dust grains are described as agglomerates of two-component core-mantle particles (Greenberg and Li, 1999a; Mann et al., 2004).

In this paper, the attention is paid to particles with a volatile ice layer coating (Notesco and Bar-Nun, 2005) on moderately absorbing organic grains. The organic materials with the refractive index $1.5+0.1i$ (Zubko and Shkuratov, 2004) fills the inner parts (core) of a particle. Although the light scattering theories for core-mantle particles are well-established and commonly available (e.g. Wickramasinghe, 1967), the approximation by homogeneous spherical targets is constantly applied to characterize optical behavior of interplanetary dust particles (since long ago, e.g. Schwehm, 1976, up to now, e.g. Greenberg and Li, 1999b; Reach et al., 2003). The reason is evidently in a simplification of theoretical derivations, an easy implementation of source codes, and in saving CPU during vast numerical runs. However, dust particles have neither spherical, nor spheroidal morphologies. This especially true for the core of a dust particle. Rather than being a symmetric object, the solid core may show a stochastic geometry. Following a statistical point of view (Sun et al., 2003) such a shape can be neatly satisfied by Gaussian particles (Battaglia et al., 1999). Many studies on non-spherical particles confirmed that the optical response of stochastically shaped obstacles may differ from that of symmetrically formed targets (like ellipsoids). It is therefore a quite reasonable motivation to evaluate how the morphology of a core may influence the resulting optical characteristics of the composite particles. Two distinct topologies: i) a homogeneous spherical particle with averaged optical properties, and ii) a Gaussian core with ice coating are compared with the aim of recognizing the optical behavior of interplanetary

dust particles during the process of vaporization. We assume here that ice is completely surrounding the solid core at large distances from the Sun. As the two-component Gaussian particle inspirals toward the Sun, the volatile coating continuously evaporates occupying the minimal surface on the core. That is, the thickness of the ice shell reduces monotonously, which is accompanied by a gradual growth of core-space interface (Fig. 1). Both the ice-space and the core-ice interfaces simultaneously vanish (ice may temporarily cover only discrete regions - cavities in the Gaussian core). On the other hand, the homogeneous sphere is modeled as an idealized mixture of ice and core materials, keeping the volume content of both constituents to be the same as in case of the Gaussian particle. We have accepted the value of $1.31{+}0.0i$ for the refractive index of water ice in the visible spectral range (e.g. Mukai et al., 1986).

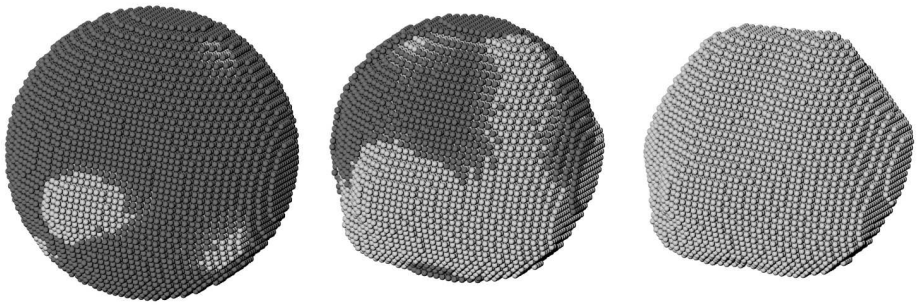

Figure 1. An model of two-component particles with volatile ice coating on a Gaussian core. The ice shell smoothly vanishes (left to right) in the process of evaporation.

2. Modeling the optical properties of two-component particles

It is well known that the particle shape has direct influence on the scattering pattern. Depending on an approach used in modeling the stochastic geometries, a set of efficient simplifications is possible in scattering calculations. Assuming that the surface deformations are small enough, the model of a perturbed sphere becomes useful to characterize the radius $a(\theta, \phi)$ of a core

$$a(\theta, \phi) = \tilde{a}\left[1 + \delta f_1(\theta, \phi) + \delta^2 f_2(\theta, \phi) + ...\right] \quad , \tag{1}$$

where $\tilde{a}$ is the radius of an unperturbed sphere, δ is a smallness parameter, and $f_n(\theta, \phi)$ are arbitrary, single valued, continuous functions satisfying the following

conditions (Yeh, 1964)

$$f_n(\theta,0) = f_n(\theta,2\pi); \qquad \sum_{n=1}^{\infty} |\delta^n f_n(\theta,\phi)| < 1 \quad . \tag{2}$$

The spherical coordinates θ and ϕ can vary over the intervals: $0 \leq \theta \leq \pi$ and $0 \leq \phi \leq \pi$. Rather recently studies have begun on spheres with surface deformations of arbitrary size (Muinonen 2000). Stochastic geometry is usually represented by Gaussian particles (Muinonen 1996). Compared with Yeh's approximation discussed above, the applicable perturbations of the Gaussian particles are "almost" arbitrary. The Gaussian shapes are very convenient to simulate real morphologies satisfying a statistical point of view (Lumme and Rahola 1998). Compared with Eqs. (1-2) the surface of a Gaussian particle is modeled as follows

$$a(\theta,\phi) = \hat{a} \exp\left[f(\theta,\phi) - \frac{1}{2}\,\beta^2\right] \quad . \tag{3}$$

The parameters $\hat{a}$ and β are the mean radius and the standard deviation of $f(\theta,\phi)$, respectively, and the spherical harmonics series $f(\theta,\phi)$ describing the three-dimensional Gaussian random sphere are expressed as follows

$$f(\theta,\phi) = \sum_{\ell=0}^{\infty} \sum_{m=0}^{\ell} P_\ell^m(\cos\theta)(A_{\ell m}\cos m\phi + B_{\ell m}\sin m\phi) \quad , \tag{4}$$

where P_ℓ^m are associated Legendre functions having the form

$$P_\ell^m = (-1)^m (1-x^2)^{m/2} \frac{d^m}{dx^m}\, P_\ell(x) \tag{5}$$

and

$$P_\ell(x) = \frac{1}{2^\ell \ell!} \left(\frac{d}{dx}\right)^\ell (x^2-1)^\ell \tag{6}$$

with $x \in \langle -1, 1\rangle$. The coefficients $A_{\ell m}$ and $B_{\ell m}$ are independent Gaussian random variables with zero means. We have simulated the Gaussian core with the radius $a(\theta,\phi)$ varying less than $\pm$ 20% (Fig. 1). The distribution and depth of both the cavities and the peaks on the surface of a Gaussian core are random. In addition to the standard Gaussian perturbed sphere we randomized also the halfwidth of convexities or concavities at the particle's surface.

If the electromagnetic radiation interacts with a homogeneous geometrically well-defined particle, the characteristics of scattered light can be calculated by the T-matrix method (Mishchenko et al., 2002). Unlike the Mie scattering theory, the T-matrix approach decomposes the electromagnetic field on a basis of functions adapted to a more-complex geometry of the scatterer. Because the surface of a Gaussian particle is described by a continuous (piecewise smooth)

function (Eq. 3), it is mathematically possible to find the T-matrix and thus to determine the characteristics of scattered light. However, the T-matrix is limited in arbitrariness of the particle shape, e.g. when ice coating occurs in discrete regions (e.g. in cavities) of the Gaussian core. Under such conditions the interfaces between the core and ice are quite complex and one needs to apply another exact solution technique. Discrete Dipole Approximation (DDA, Draine and Flatau 1994) is widely employed to calculate scattering behavior of composite particles with various geometries and material configurations. In principle, DDA is a finite element method in which the continuum target is replaced by an array of point dipoles (Purcell and Pennypacker 1973). When the particle is built up by many cubes (dipoles) with a lattice spacing d significanly smaller than the wavelength λ of an incident radiation, the scattering problem is translated into a problem of retrieval of the dipole moments $\boldsymbol{p_i}$ for every single cell. To get $\boldsymbol{p_i}$ one must solve the system of $3N$ complex linear equations (Singham and Bohren 1987)

$$\frac{1}{\epsilon_0} \sum_{j=1}^{N} \mathbf{A}_{ij}\ \boldsymbol{p_j}(\boldsymbol{r_i}) = \boldsymbol{E^{inc}}(\boldsymbol{r_i}) \tag{7}$$

where ϵ_0 is the electric permittivity of free space, N is the number of cells, $\boldsymbol{r_i}$ is the position of the central point of the i-th cell, $\boldsymbol{E^{inc}}(\boldsymbol{r_i})$ is the incident electric field at the position $\boldsymbol{r_i}$, and $\mathbf{A}_{ij}$ is a 3×3 matrix whose non-diagonal components characterize dipole-dipole interactions and diagonal components refer to self interactions. Once the dipole moments $\boldsymbol{p_i}$ are determined (solving Eq. 7), the calculation of the external (scattered) fields is a straightforward procedure; and the optical characteristics like extinction, scattering, and absorption cross sections, or a phase function, or linear polarization can be obtained. Draine and Flatau (2004) released the public-domain DDA code (called DDSCAT), which uses fast Fourier transform techniques (FFT) to evaluate matrix-vector products $\mathbf{A}_{ij}\ \boldsymbol{p_j}$. We used DDSCAT to calculate scattering properties of a Gaussian core with ice coating. To guarantee the numerical results will be sufficiently accurate (i.e. the calculation error for intensities and other angular optical characteristics will vary within several percents), the product of $|m|k_0 d$ must be smaller than ≈ 0.5, i.e. the phase should vary less than 0.5 radian between individual dipoles. Here k_0 is the wave number in vacuum, and m is the complex refractive index of the particle.

With the DDA approach every cell can have its own dielectric properties, which is one of the most important advantages of this computing technique. An arbitrarily shaped and small heterogeneity can be therefore incorporated into our particle model. But, the DDA calculations are time- and memory-consuming when the particle size increases. This is because rapid growth of the system of equations (the system consists of $3N$ linear equations as it comprises expressions for all three coordinates). The number of cells N needed to satisfy a more conservative criterion $|m|k_0 d < 0.5$ is a function of the particle volume V. Because the simulated particle may have a complex form it is convenient to

introduce a characteristic radius of an equal volume sphere

$$a_m = \left(\frac{3V}{4\pi}\right)^{1/3} \quad . \tag{8}$$

The scattering characteristics are then expressed in terms of a dimensionless size parameter x

$$x = \frac{2\ \pi\ m\ a_m}{\lambda} = \frac{2\ \pi\ m\ d}{\lambda}\left(\frac{3V}{4\pi}\right)^{1/3} \quad . \tag{9}$$

In general, the DDA works well when the effective radius a_m of volume equivalent sphere doesn't exceed the value $\approx 2.5\lambda$. We considered the wavelength $\lambda = 0.525\ \mu m$, thus the DDA provides correct results for particles with sizes less than approximately 1-2 μm. These particles are optically active, i.e. they show enhanced scattering features in the visible spectral range and a large amount of ground-based astronomical observations are performed in this spectral region. It is well recognized that (sub)micrometer sized particles are produced by comets - this fact was deduced when analysing polarized light of the continuum. For instance, the spectral energy distribution in the coma of the comet Hale-Bopp was dominated by scattering and thermal emission from very small submicron sized dust grains (Williams et al., 1997). In general, particles of various sizes coexist in a dusty coma (Dollfus, 1989).

Our computations were carried out for composite particles with original sizes ranging from 0.4 up to $\approx 1.5\ \mu m$ - to comply with observations of dust tails for various comets (Swamy, 1986). The ratio of coat to core volumes is considered to be 6/4 at the beginning of vaporization processes, i.e. the ice filling is 60%, while the core represents only 40% of the total volume of the particle. As evaporation continues the coating vanishes, so at the end of this process the ice disappears completely. The light scattering calculations for such model of the Gaussian core with ice coating is straightforward when using DDA. Because of the complexity of modeled particles, in both characterization and calculating their resulting scattering, it is usually desirable to characterize the system using simple, homogeneous particles. Nevertheless, an additional treatment is needed before running attractive Mie calculations (Bohren and Huffman, 1998). The rigorous Mie theory is strictly applicable to homogeneous spheres, thus some kind of manipulation is necessary to determine the mean refractive index of the particle. At present, a set of effective medium theories (EMTs) is available to calculate the dielectric function of multicomponent media (Choy, 1999). Typically these methods only work well if the inclusions are sufficiently small compared to the wavelength. Generally speaking, EMTs approximate the optical properties of the inhomogeneous scatterer by those of a homogeneous particle of the same shape. The advantage of an EMT is that a homogeneous particle can be calculated much more easily and rapidly than a heterogeneous particle. One of the easiest EMTs is volume (mass) weighted mixing (Kolokolova et al., 2001)

for which the resulting refractive index m is given as $m = \sum_j m_j f_j$. here m_j stands for the refractive index of the j-th species and f_j is its volume fraction. It should be noted that the volume-averaged mixing rule has no theoretical foundation, therefore more convenient approximations have to be applied. The most commonly used EMTs are the Maxwell-Garnett theory (Maxwell Garnett, 1904) and the Bruggeman theory (Bruggeman, 1935). In these theories, the domains dispersed in a continuous host of another material form so-called separated grain structure. We employed the Bruggeman theory in which the mean dielectric function $\bar{\epsilon} = \bar{\epsilon}_r \ + \ i \ \bar{\epsilon}_i$ of the particle is calculated as follows

$$\sum_{j=1}^{2} f_j \ \frac{\bar{\epsilon} - \epsilon_j}{2 \ \bar{\epsilon} + \epsilon_j} = 0 \tag{10}$$

where pairs (ϵ_1, f_1) and (ϵ_2, f_2) represent the dielectric functions and volume fractions of the core and shell, respectively. It is obvious that the relation $f_1 = 1 - f_2$ must be fulfiled. The mean refractive index of the homogeneous sphere supplying the two-component particle is

$$\bar{m} = \sqrt{\frac{\sqrt{\bar{\epsilon}_r^2 + \bar{\epsilon}_i^2} + \bar{\epsilon}_r}{2}} \ + \ i \sqrt{\frac{\sqrt{\bar{\epsilon}_r^2 + \bar{\epsilon}_i^2} - \bar{\epsilon}_r}{2}} \quad . \tag{11}$$

However, it must be taken into account that any EMT involves heavy approximations on the dielectric functions that may not be completely satisfied (Iatì et al., 2004). As inhomogeneous particles (e.g. cometary dust) are frequently replaced by spherical homogeneous obstacles (hoping that the optical behavior of these particles is not very different from reality) it is necessary to verify the applicability of this approximation. The calculated optical properties of both, the homogeneous particles and the real two-component particles, are compared in the next section.

3. Scattering features of composite volatile particles

A statistically large ensemble of dust particles grouped into a cloud consists of randomly shaped, sized and oriented grains. We are applying a concept of Euler angles (Φ, θ, and Ψ) to characterize an orientation of every single grain with respect to the laboratory reference frame. All orientations of the particles are implicitly equiprobable and thus the orientation distribution function of the whole dust population is uniform with respect to the chosen system of Euler angles. Any orientationally averaged optical quantity of a monodisperse set of equally shaped particles is then easily determined by a triple integral

$$\langle \ Q(a, \lambda, m) \ \rangle = \frac{1}{8\pi^2} \int_0^{2\pi} d\Phi \int_0^{\pi} \sin\theta \ d\theta \int_0^{2\pi} \ Q(\Phi, \theta, \Psi, a, \lambda, m) \ d\Psi \quad . \tag{12}$$

Numerical simulations on composite particles with the Gaussian core with volatile ice coating are done by means of Eq. (12), where Q supplies one of the following optical quantities: an efficiency factor for scattering Q_{ext} and backscattering Q_{bk} as well as the polarization P and the scattering phase function S_{11} (Bohren and Huffman, 1998). Admittedly, the time-consuming integrations in Eq. 12 are not needed for Mie spheres.

3.1. Efficiency factors for scattering and backscattering

A useful concept in describing the optical properties of the dust particles utilizes cross sections (Quirantes and Delgado 2001). However, cross sections may change over several orders of magnitude. These physical quantities are therefore inconvenient for a graphical presentation. It is much more effective to deal with efficiency factors for scattering Q_{sca}, and backscattering Q_{bk}, each of them defined as a ratio of the corresponding cross section to the projection area of a particle.

The scattering ability of a particle is often characterized by an efficiency factor for scattering Q_{sca}. The results of numerical calculations of Q_{sca} for two-components Gaussian particles and homogeneous spheres are presented in Fig. 2. It needs to be highlighted that the evaporation processes are accompanied by monotonous reduction of the mean effective radius of a particle. Thus, if the volume fraction of the ice is reduced from 60% to 0%, the original radius of the particle decreases by a factor of 0.74 (from a to a_0, where a is the actual particle radius, and a_0 is the particle's radius at the end of the vaporization process). In the case of scattering efficiency it is traditional to draw Q_{sca} as a function of the size parameter x (Eq. 9) instead of the particle radius a. Scattering efficiency of very small particles (for which $a_0 \lesssim 0.15\ \mu m$) decreases steeply if ice content diminishes. This trend is kept for Gaussian as well as for homogeneous particles. However, the particles comparable to the wavelength of observation ($a_0 \gtrsim 0.2\ \mu m$) show more complex behavior. First of all we notice that the Gaussian particles with $a_0 \gtrsim 0.2\ \mu m$ scatter less efficiently than volume equivalent homogeneous spheres. When the size of a scatterer becomes comparable to λ, the interference effects strongly influence the spatial redistribution of scattered light. Due to destructive interference the amplitudes of scattered electric field may show deep minima in some directions and this can change dramatically with a slight modification of the particle size. The absorbing material has a centered position in the Gaussian particle, while such a material is spread over the whole volume of a homogeneous particle. Light transmitted into homogeneous sphere decreases because the refractive indices of the particle and those of the outer space differ significantly. The light beams penetrating through the large homogeneous sphere ($a_0 \gtrsim 0.5\ \mu m$) are then attenuated already in the shell, and this is accompanied by rapid reduction of amplitudes of the electric field. On the other hand, the ice surrounding the Gaussian core is a non-absorbing constituent, implying that the discontinuity of material constants at the particle-

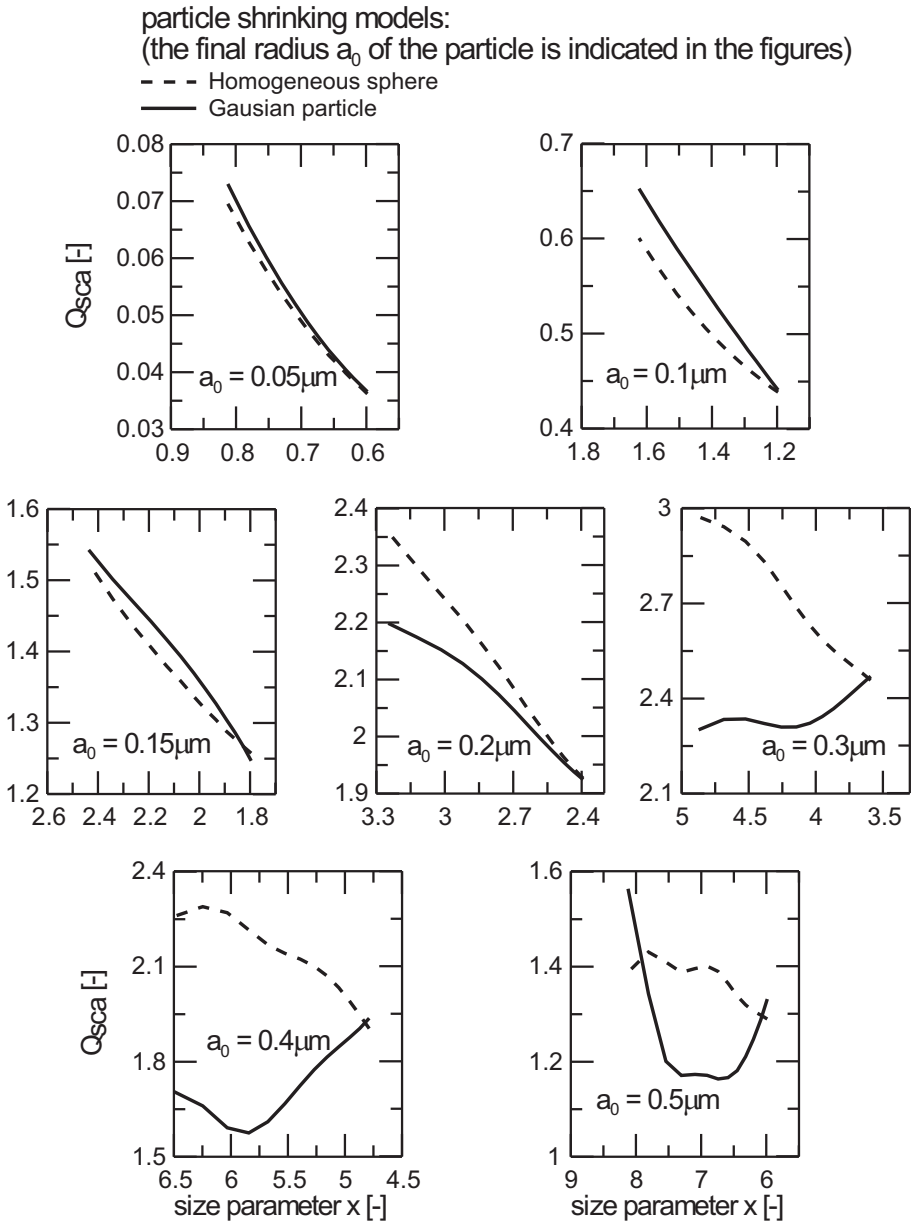

Figure 2. The efficiency factor for extinction Q_{ext} as a function of the size parameter x for two different particle topologies: a Gaussian core with ice coating and a homogeneous sphere. Evaporation processes, in which the particle loses the ice, are characterized by continuous decrease of the size parameter x.

space interface is not so large. Consequently, the thicker ice coating on a large Gaussian core ($a_0 \gtrsim 0.5\ \mu m$), the more enhanced scattering efficiency. This is in exact agreement with the results presented in Fig. 2 for Gaussian particles. Scattering efficiency of moderately sized Gaussian particles can, however, grow during evaporation processes.

In principle, the independent ensembles of dust particles of different origin can be characterized by quite similar values of $\langle Q_{sca} \rangle$, so we are currently unable to differentiate the particles only from their overall scattering ability. Some astrophysical methods of the characterization of particle systems are based on an analysis of backscattering signals which have relation to the so-called efficiency factor for backscattering Q_{bk}. The quantity Q_{bk} is a differential cross section for backscattrering divided by the projection area of the particle. Q_{bk} yields the supplementary information on microphysics of the scattering particles. As expected, the topology of the particle has a minor influence on Q_{bk} in the Rayleigh approximation, i.e. when particle sizes are below the Mie limit (Fig. 3; $a_0 < 0.05\ \mu m$). As the particle size approaches that of the Mie limit, no preferred trend of Q_{bk} is recognized when analyzing the processes of ice loss. The ripple structure of the efficiency factor for backscattering has relation to mutual evolution of both the optical properties and size of the particles. Therefore the transitions from decreasing to increasing behavior of Q_{bk} for Gaussian and homogeneous particles corelate together. In general, large homogeneous spheres show enhanced backscattering, while two-component particles scatter less efficiently in the backward direction. This is for the same reason as discussed in the case of Q_{sca}. In real situations, the internal topology of the cosmic dust particles is notoriously unknown. Therefore homogeneous spheres are often employed to simplify modeling the particle populations. Our results shown that such approximation may lead to a significant overestimation of the backscattering ability of the particles (note that Q_{bk} is drawn on a logarithmic scale in Fig. 3). Under these conditions the interpretation of backscattered signals can be incorrect (e.g. the retrieval of microphysical properties of dust particles will be faulty).

3.2. Intensities and polarization of scattered light

The phase function S_{11} for a single non-spherical particle depends on its orientation with respect to the direction of incidence of the radiation and on the particle's characteristics. In spite of this fact, a statistically large system of randomly oriented particles manifests the scattering behavior depending on a scattering angle θ. The scattering angle θ is simply the angle between the incident beam and the scattered beam ($\theta = 0^\circ$ for forward scattering, $\theta = \pi$ for backscattering). Measurements of the scattered light in the visible spectral region appear to be a good source of information on interplanetary particles, e.g. on cometary dust. The presence of small or large particles in a dusty coma can be recognized when analyzing the spectral behaviour of the intensity of the scat-

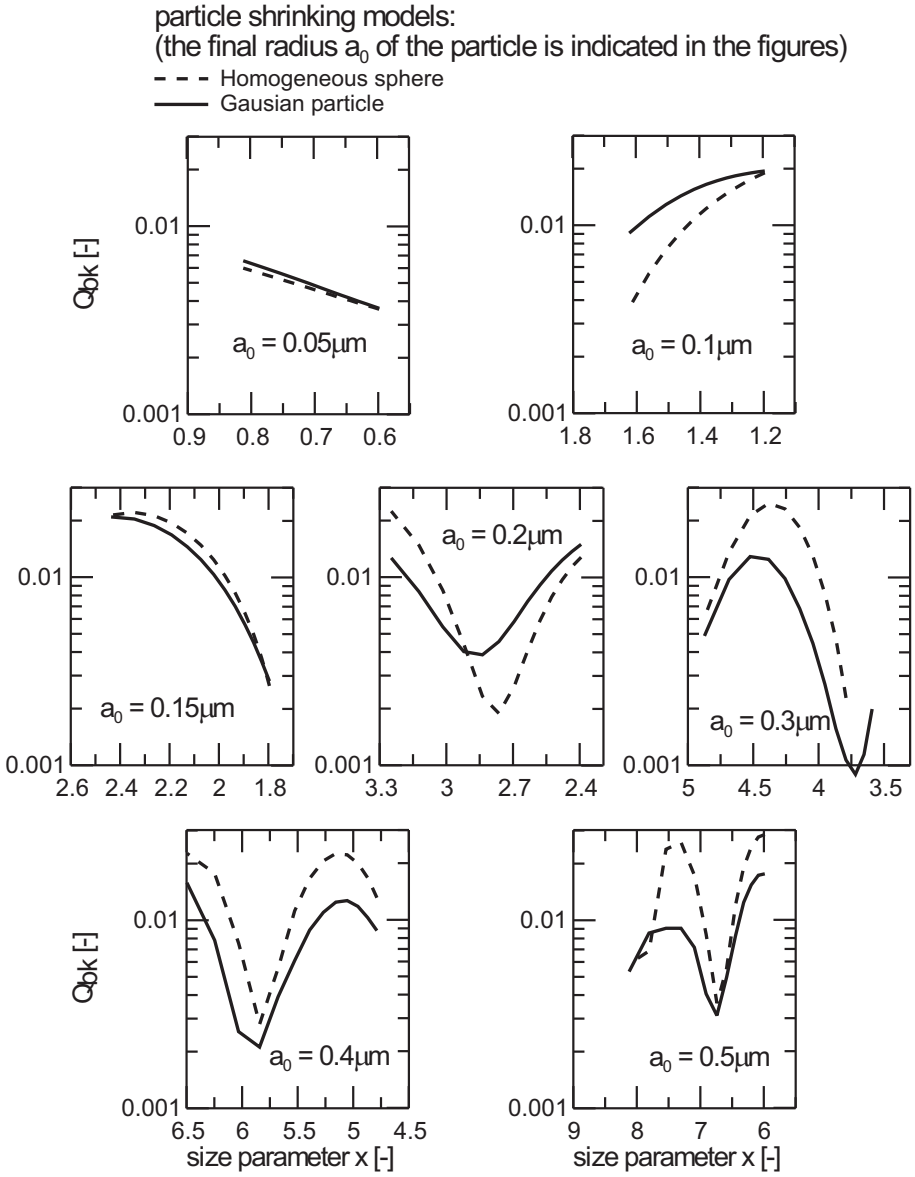

Figure 3. The efficiency factor for backscattering Q_{bk} as a function of the size parameter x for two different particle topologies: a Gaussian core with ice coating and a homogeneous sphere. Evaporation processes, in which the particle loses the ice, are characterized by continuous decrease of the size parameter x.

tered light. The advantage of this method is that we do not need to handle the absolute values of the intensities (Kocifaj et al., 2002). Nevertheless, the results of the retrieval algorithm may be inaccurate if inappropriate optical models of the scattering particles are employed. It is therefore important to recognize how much the scattering intensities for idealized spherical particles differ from those for a Gaussian core with volatile ice coating. The results of numerical runs are presented for particles with initial radii 0.14 μm, 0.41 μm, and 0.68 μm. The sizes of these particles decrease because of ice loss, so at the end of the evaporation process the corresponding core radii are as follows: $a_0 = 0.1$ μm (Fig. 4), $a_0 = 0.3$ μm (Fig. 5), and $a_0 = 0.5$ μm (Fig. 6), respectively.

The particles smaller than the wavelength of an incident radiation have similar scattering patterns (Fig. 4) independent of particle morphologies. This is because of the Rayleigh approximation. The scattering functions S_{11} for Gaussian particles and homogeneous spheres are in good agreement, especially in forward directions. The biggest discrepancies occur in the backscattering region when the ice coat is quite thick. In this case, no core-space interface is present in the Gaussian model, and thus the sunbeams transit much easier into a particle coated with the ice shell. On the other hand, the homogeneous sphere behaves more-less like an absorbing obstacle (because the absorbing material is homogeneously distributed over the whole particle volume). Such particles have typically reduced backscattered signals. Particles with sizes comparable to the wavelength of incident radiation show intensive forward scattering if they are considered to be homogeneous spheres (as illustrated in Figs. 5 and 6). This fact is physically reasonable. It is well known that the physical response of any matter placed in an external field is the induction of a net dipole moment. Splitting the particle into an array of very small cells one can argue that every cell undergoes polarization depending only on the local field at the cell (DeVoe, 1964). The electric polarization (the average electric dipole moment per a unit volume) of the particle and the dipole moment $\boldsymbol{p}_i$ of an the i-th cell are related as follows

$$\mathbf{P} = \frac{1}{V}\sum_{i=1}^{N} \boldsymbol{p}_i \equiv n\tilde{\boldsymbol{p}} \quad , \tag{13}$$

where $\tilde{\boldsymbol{p}}$ is an average dipole moment of a single cell, N is the number of cells, and V is the total volume of the particle. Dipole moments $\boldsymbol{p}_i$ can be obtained as a solution of the electromagnetic problem for internal fields. Knowing $\boldsymbol{p}_i$, the calculation of the optical properties, like cross sections for extinction and absorption, is easy:

$$C_{ext} = \frac{4\pi k_0}{|\mathbf{E}_0^{inc}|^2}\ \frac{1}{4\pi\epsilon_0}\ \sum_{i=1}^{N} \mathrm{Im}(\mathbf{E}_i^{inc})^* \cdot \boldsymbol{p}_i \quad , \tag{14}$$

$$C_{abs} = \frac{4\pi k_0}{|\mathbf{E}_0^{inc}|^2}\ \frac{1}{4\pi\epsilon_0}\ \sum_{i=1}^{N} \left\{ \mathrm{Im}[\boldsymbol{p}_i \cdot (\alpha_i^{-1})^*\ \boldsymbol{p}_i^*] \ -\ \frac{2}{3}k_0^3|\boldsymbol{p}_i|^2 \right\} \quad , \tag{15}$$

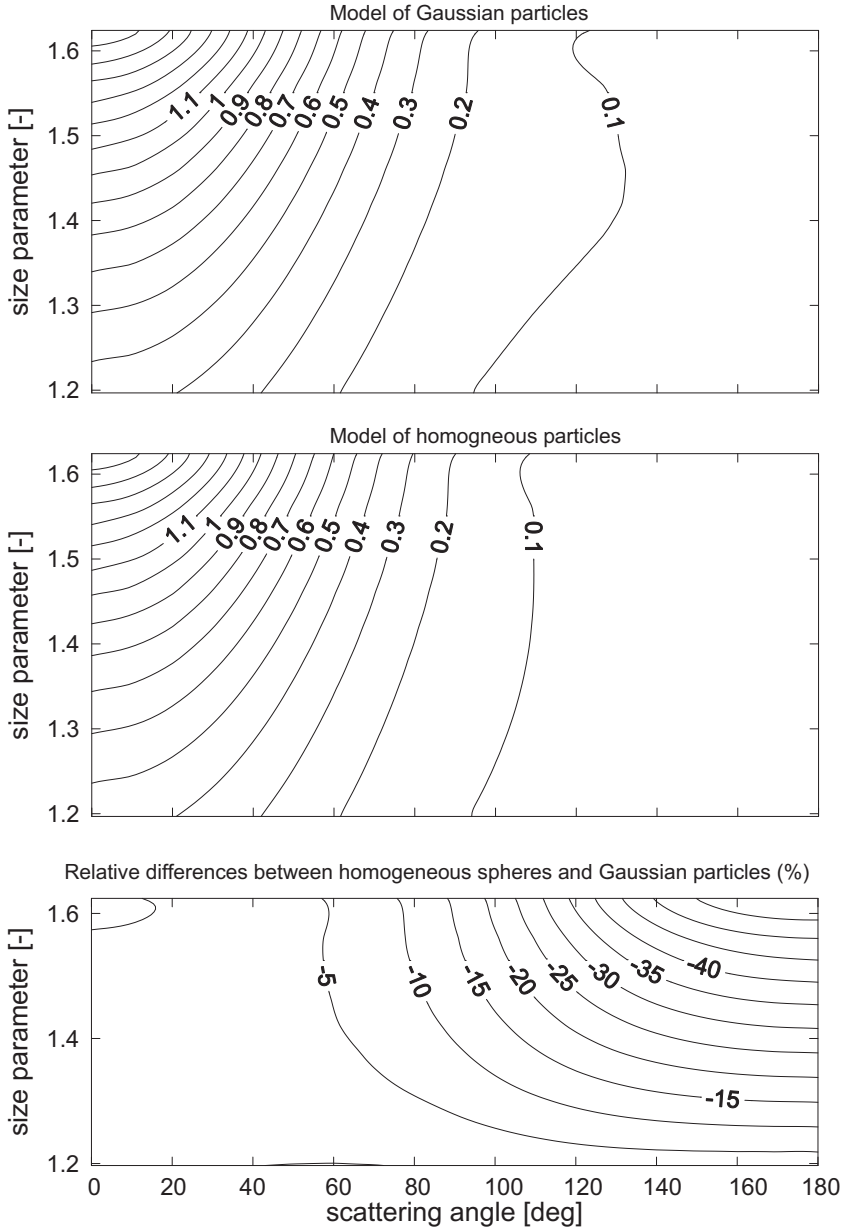

Figure 4. Dependency of scattering intensities S_{11} on the scattering angle and the size parameter x for evaporating particles with core radius $a_0 = 0.10\ \mu m$). Top panel: $S_{11}(Gp)$ for a *G*aussian *p*article with ice coating. Middle panel: $S_{11}(hs)$ for a *h*omogeneous *s*phere. Bottom panel: relative differences of scattering intensities calculated as follows: $100 \times [S_{11}(hs) - S_{11}(Gp)]/S_{11}(Gp)$.

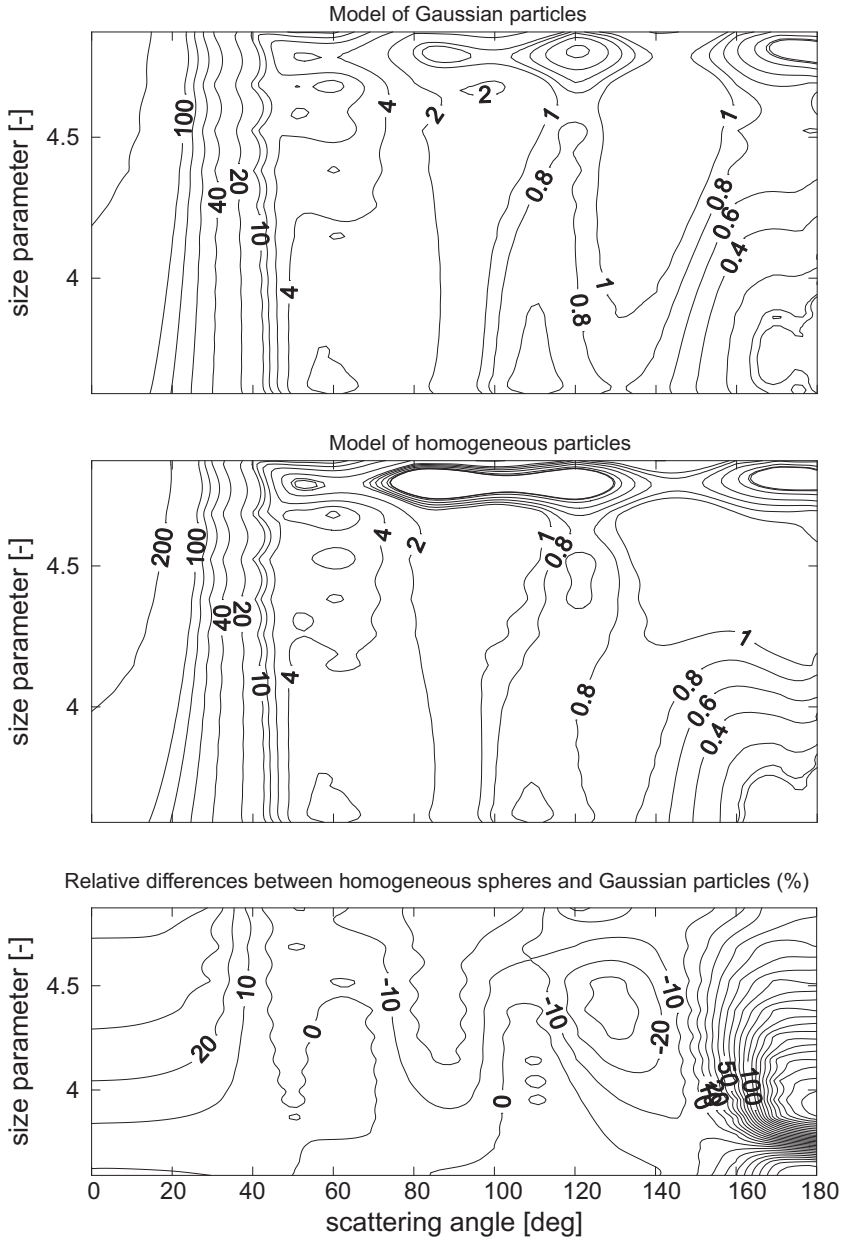

Figure 5. Dependency of scattering intensities S_{11} on the scattering angle and the size parameter x for evaporating particles with core radius $a_0 = 0.30\ \mu m$). Top panel: $S_{11}(Gp)$ for a *G*aussian *p*article with ice coating. Middle panel: $S_{11}(hs)$ for a *h*omogeneous *s*phere. Bottom panel: relative differences of scattering intensities calculated as follows: $100 \times [S_{11}(hs) - S_{11}(Gp)]/S_{11}(Gp)$.

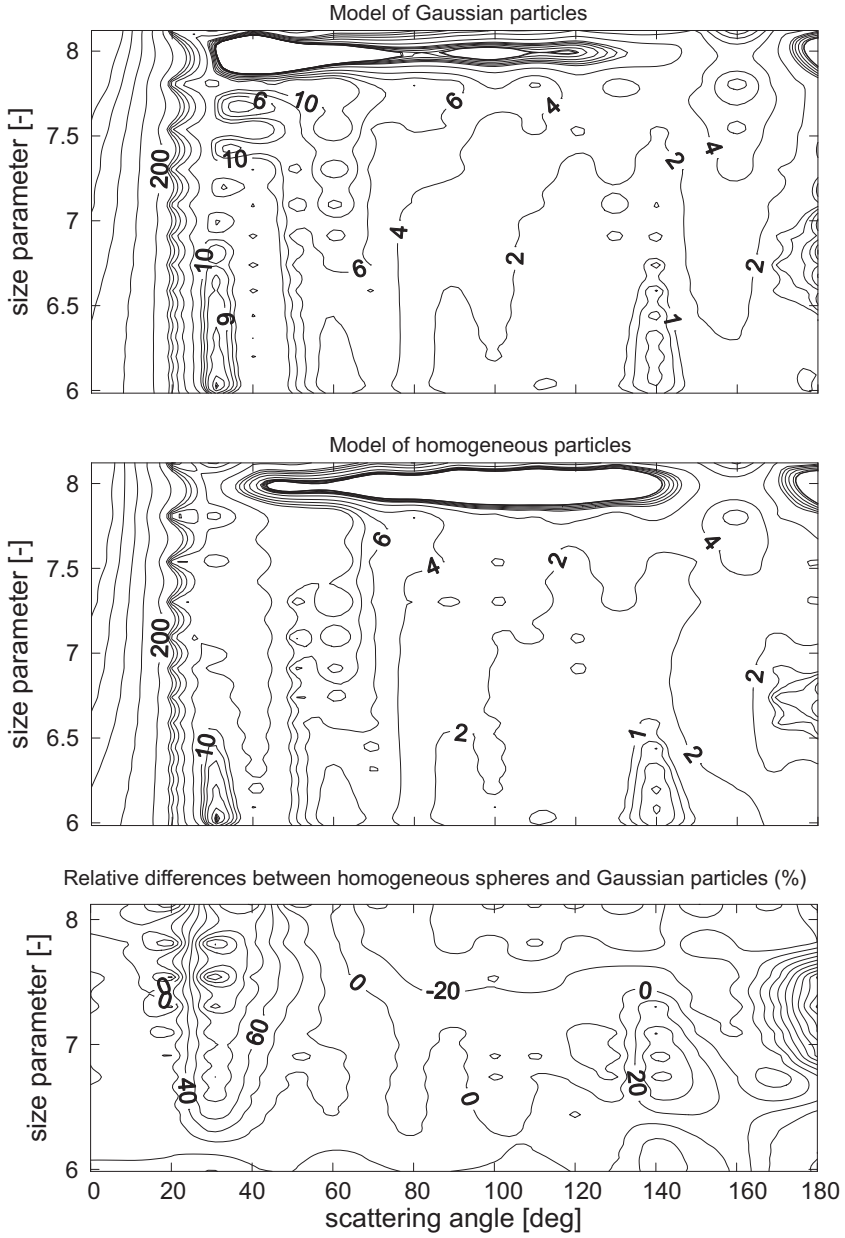

Figure 6. Dependency of scattering intensities S_{11} on the scattering angle and the size parameter x for evaporating particles with core radius $a_0 = 0.50\,\mu m$). Top panel: $S_{11}(Gp)$ for a *G*aussian *p*article with ice coating. Middle panel: $S_{11}(hs)$ for a *h*omogeneous *s*phere. Bottom panel: relative differences of scattering intensities calculated as follows: $100 \times [S_{11}(hs) - S_{11}(Gp)]/S_{11}(Gp)$.

where $\mathbf{E}_i^{inc}$ is the incident electric field at the position of the i-th cell and $\mathbf{E}_0^{inc}$ is the amplitude of this field, and α_i is so-called polarizability. When the particle is built up by many cells significanly smaller than the wavelength of an incident radiation, the Clausius-Mossotti prescription would apply (Sivasubramanian et al., 2005) and the α_i acquires the form

$$\alpha_i = \frac{3}{n}\,\frac{m^2-1}{m^2+2} \quad . \tag{16}$$

The scattering function has a direct relation to the differential scattering cross section $dC_{sca}/d\Omega$ (where $d\Omega$ is an elementary solid angle). This quantity can be derived from $C_{sca} = C_{ext} - C_{abs}$ (consult Eqs. (14-15). It is now obvious that the configuration of dipole moments $\boldsymbol{p}_i$ has direct impact on S_{11}. A dipole moment is proportional to the product of polarizability and incident field; therefore, the larger refractive index, the greater dipole moments are induced. The enhanced scattering ability found for the model of a homogeneous sphere can be therefore ascribed to the following mechanism: when the high-refractive-index components that produce greater dipole moments are located at the edges of the particle, rather than concentrated in its center, their contributions to the scattering amplitudes in the backscatter region have acquired greater phase differences than if they are concentrated at one location (Gangl et al., 2008). In the backscatter, these phase differences translate to destructive interference that lowers the intensity (this is what we observed already in Fig. 4). In particular, the refractive index of the core is considerably higher than that of ice coat. The Bruggeman theory leads to averaging of the dielectric function over whole volume of the particle, thus implying an increase of the refractive index at the edge of a homogeneous spherical particle.

Another important physical quantity that can offer information on the nature and size of particles is the polarization P of the scattered radiation (Swamy, 1986). However, applicability of polarization measurements is restricted as these need to be taken for a few scattering angles. Generally, the larger the angular interval, the more valuable the information content. When dealing with cometary dust it must be taken into account that the optical data need to be be collected during a relatively large time period, generally at different comet-Sun distances. As the cometary activity may significantly change with time, the inconsistencies in the data become apparent.

The values of P for small homogeneous spheres do not differ much from those obtained for Gaussian particles (Fig. 7). However, already small particles of various forms can be differentiated from their polarization data if the ice coating is quite thick and the measurements are done at large scattering angles ($\theta \approx 120 - 150^\circ$). The information content of both, the phase function and polarization is sufficient to retrieve microphysical properties of particles with sizes comparable to, or larger than, the wavelength of incident radiation (Figs. 8-9). The biggest discrepancies between polarization features of homogeneous spheres

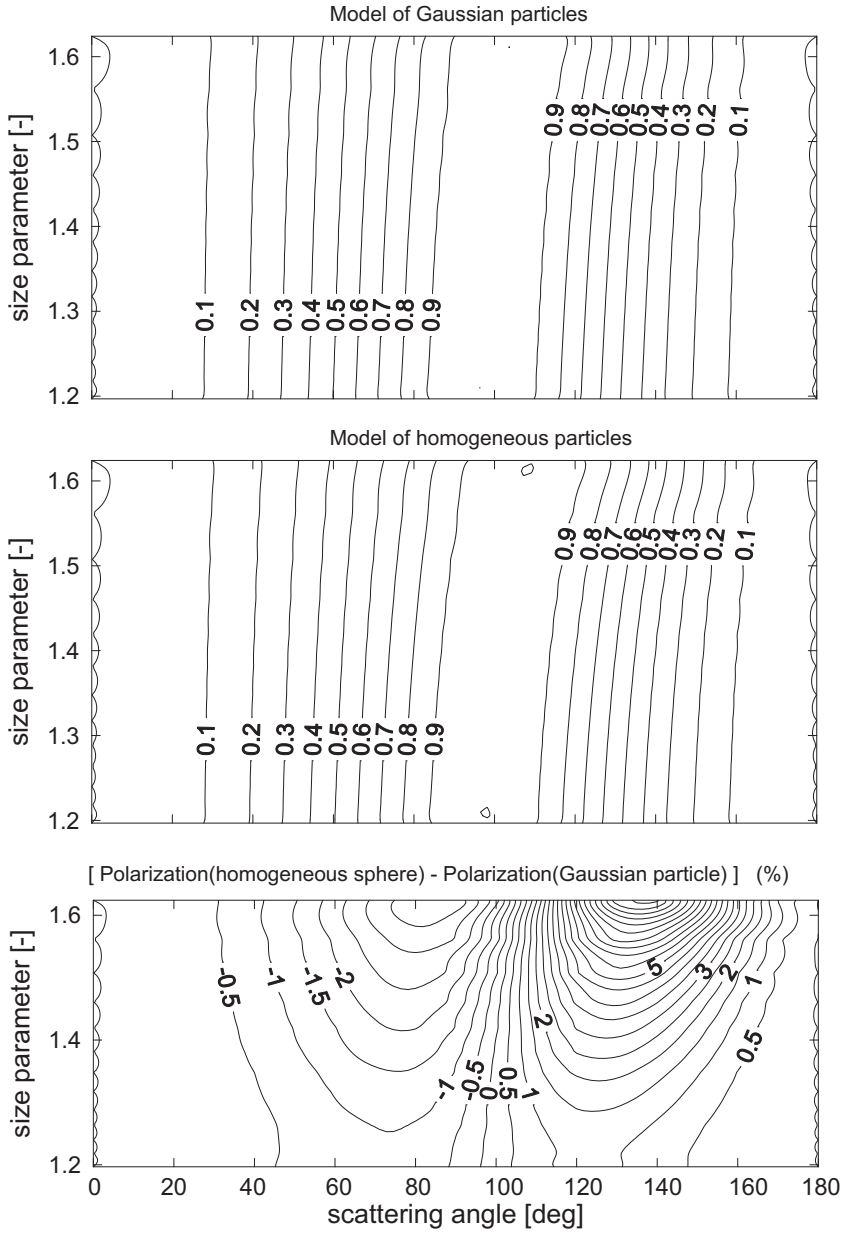

Figure 7. Linear polarization P as a function of the scattering angle and the size parameter x for evaporating particles with core radius $a_0 = 0.10\ \mu m$). Top panel: $P(Gp)$ for a *G*aussian *p*article with ice coating. Middle panel: $P(hs)$ for a *h*omogeneous *s*phere. Bottom panel: absolute differences of linear polarizations calculated as follows: $P(hs) - P(Gp)$].

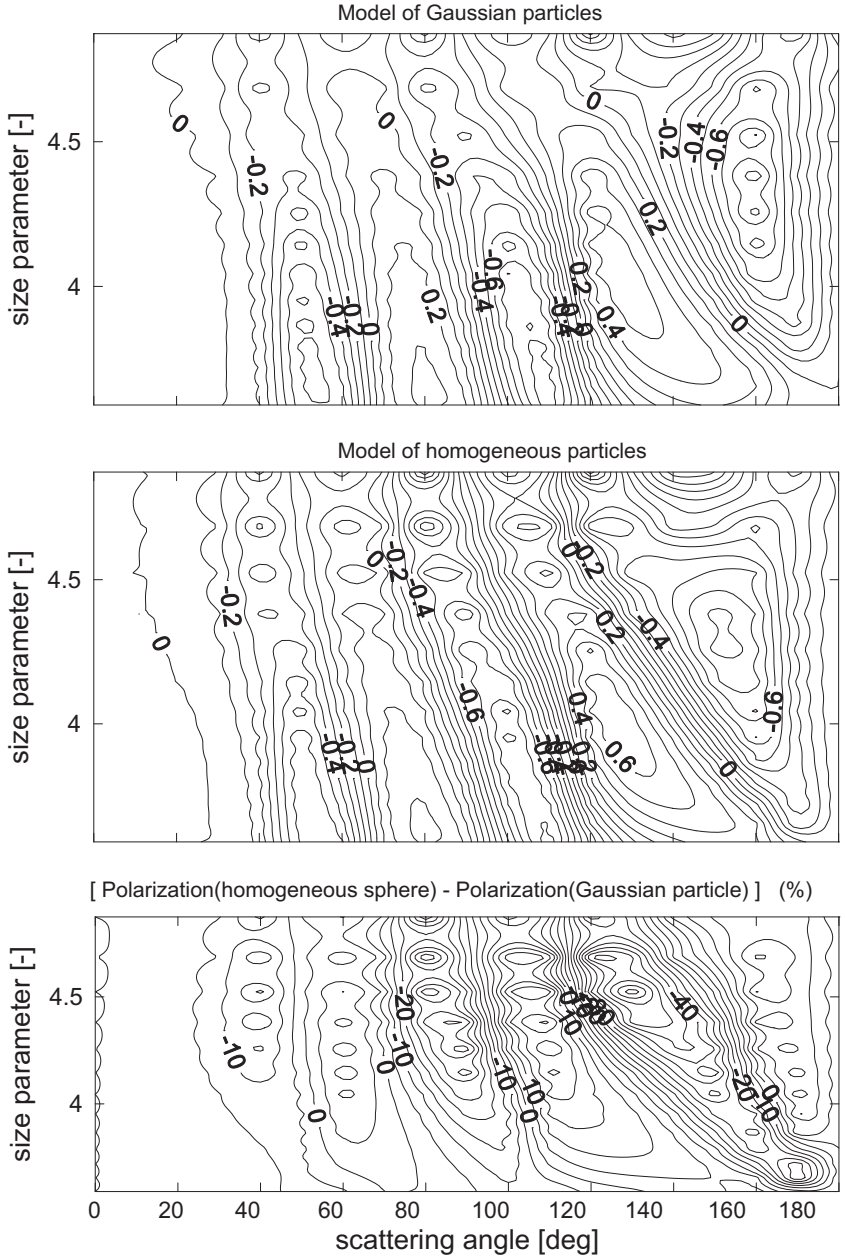

Figure 8. Linear polarization P as a function of the scattering angle and the size parameter x for evaporating particles with core radius $a_0 = 0.30\ \mu m$). Top panel: $P(Gp)$ for a *G*aussian *p*article with ice coating. Middle panel: $P(hs)$ for a *h*omogeneous *s*phere. Bottom panel: absolute differences of linear polarizations calculated as follows: $P(hs) - P(Gp)$].

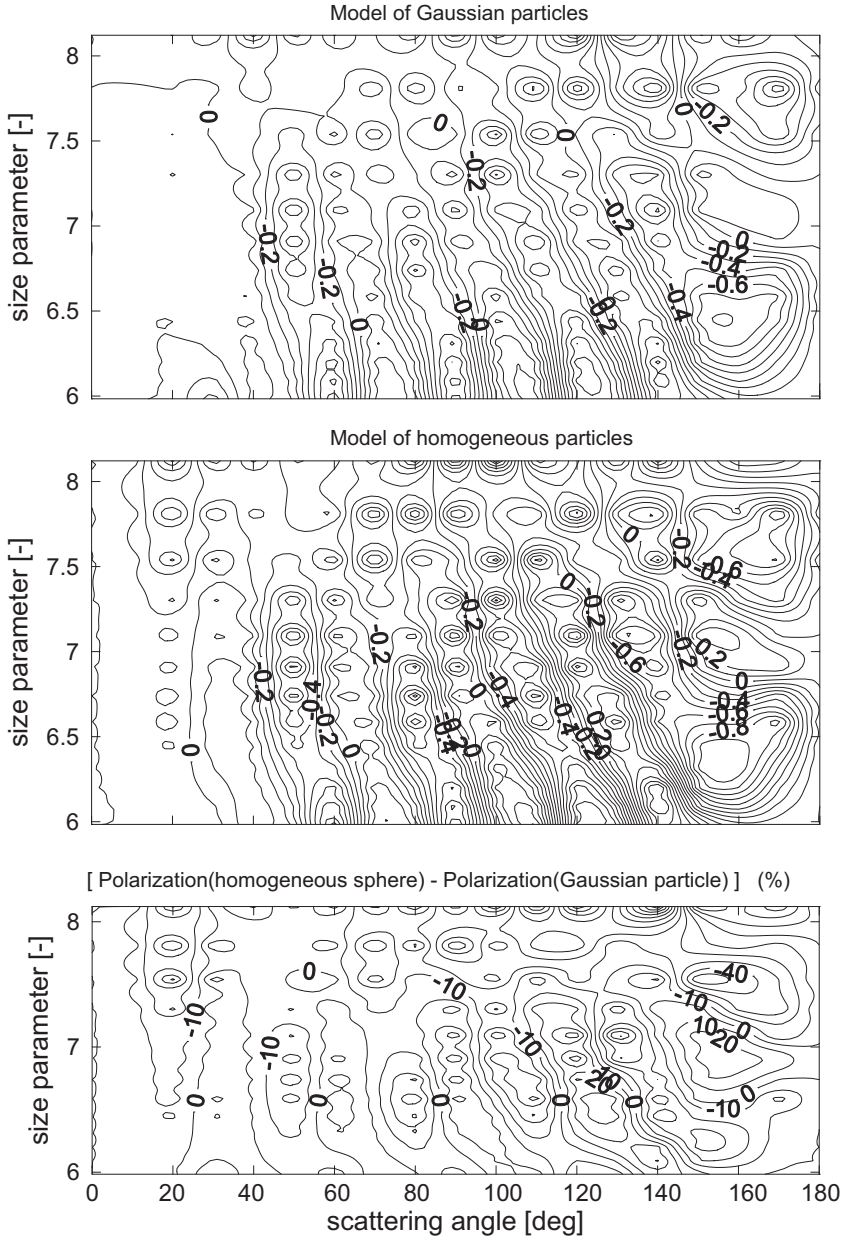

Figure 9. Linear polarization P as a function of the scattering angle and the size parameter x for evaporating particles with core radius $a_0 = 0.50\ \mu m$). Top panel: $P(Gp)$ for a *G*aussian *p*article with ice coating. Middle panel: $P(hs)$ for a *h*omogeneous *s*phere. Bottom panel: absolute differences of linear polarizations calculated as follows: $P(hs) - P(Gp)$].

and Gaussian particles are found in backward directions. The number of subsidiary peaks of P increases rapidly with the size of a particle. Concurrently, the positions of P may change even if morphological and/or topological alternations of the particles are small. Therefore the polarization P is a very valuable indicator of particle's microphysical properties. The results presented in Figs. (8-9) unambiguously illustrate the errorness of the simple Mie approximation when analysing the optical properties of realistically shaped and composite cosmic dust particles.

4. Concluding remarks

The interplanetary dust particles are still unfrequently modeled as composite aggregates and rather than being studied by complex light scattering tools (like T-matrix, or DDA) they are supplied by homogeneous spheres for which Mie theory is exactly applicable. This kind of approximation can be inadequate even if particles have shapes not very different from spheres. We have simulated two-component particles usually supplying the cometary dust. These particles contain a solid inclusion surrounded by an ice shell which diminishes due to evaporation or sputtering effects. The optical properties of such system continuously change, indicating the evolving scattering responses of the system. We have studied particles with two different topologies: a) the more realistic Gaussian core with ice coating, and b) the very simple model of a homogeneous sphere. It was shown that scattering abilities of both types of particles may significantly differ, especially when the particle size is comparable to, or larger than, the wavelength of an incident radiation. In principle, the homogeneous spheres scatter more efficiently than Gaussian particles. The absorbing material is distributed homogeneously over the volume of a spherical particle, thus implying an unfavoured beams' transition into the inner parts of large particles. In the same time, the spherical particles scatter preferrably into forward directions. Polarization features of both morphological systems are quite complex, and they are definitely distinguishable. This fact has an important consequence in the identification of the microphysical characteristics of dust particles. Bringing the polarization and scattering measurements together, various particles occuring in space can be recognized.

It would be advisable to verify these results with those obtained under laboratory conditions. However, such a comparison makes sense only if the laboratory particles are of the same size, shape, topology and composition as the numerically analyzed particles. However, it is traditionally difficult to fulfil these conditions except for special situations, e.g. when dealing with calibrated samples of manufactorable particles (like latex polymerized spheres). Some comparative studies on irregularly shaped composite particles and corresponding spheres were presented in Gangl et al. (2008) and Kocifaj et al. (2006), but the dynamical aspects were out of scope of these papers.

Acknowledgements. This work has been supported by the Scientific Grant Agency VEGA (grant No. 1/3074/06) and by the Slovak Academy of Siences (grant No. 350/OMS/Fun/07 - as part of DAAD project Nr. D/07/01266).

References

Battaglia, A., Muinonen, K., Nousiainen, T., Peltoniemi, J.I.: 1999, *J. Quant. Spectrosc. Radiat. Transfer* **63**, 277

Bohren, C.F., Huffman, D.R.: 1998, *Absorption and Scattering of Light by Small Particles*, Wiley-VCH, Weinheim

Bruggeman, D.A.G.: 1935, *Annalen der Physik* **24**, 636

Choy, T.C.: 1999, *Effective Medium Theory. Principles and applications*, Clarendon Press, Oxford

Davidsson, B.J.R., Gutiérrez, P.J.: 2006, *Icarus* **180**, 224

DeVoe, H.: 1964, *J. Chem. Phys.* **41**, 393

Dollfus, A.: 1989, *Astron. Astrophys.* **213**, 469

Draine, B.T., Flatau, P.J.: 1994, *J. Opt. Soc. Am. A* **11**, 1491

URL: Draine, B.T., Flatau, P.J. 2004. "User Guide for the Discrete Dipole Approximation Code DDSCAT.6.1", `http://arxiv.org/abs/astro-ph/0409262`

Dumont, R., Levasseur-Regourd, A.Ch.: 1988, *å* **191**, 154

Flynn, G.J.: 1994, *Planet. Space Sci.* **42**, 1151

Gangl, M., Kocifaj, M., Viden, G., Horvath, H.: 2008, *Atmosph. Environ.* **42**, 2571

Greenberg, J.M., Li, A.: 1999a, *Adv. Space Res.* **24**, 497

Greenberg, J.M., Li, A.: 1999b, *Planet. Space Sci.* **47**, 787

Handa, Y.P., Klug, D.D.: 1988, *J. Phys. Chem.* **92**, 3323

Holmes, E.K., Dermott, S.F., Gustafson, B.Å.S., Grogan, K.: 2003, *Astrophys. J.* **597**, 1211

Iatì, M.A., Giusto, A., Saija, R., Borghese, F., Denti, P., Cecchi-Pestellini, C: 2004, *Astrophys. J.* **615**, 286

Kapišinský, I.: 1984, *Contrib. Astron. Obs. Skalnaté Pleso* **12**, 99

Klačka, J.: 2004, *Celest. Mech. Dyn. Astr.* **89**, 1

Kocifaj, M., Gangl, M., Kundracík, F., Horvath, H., Videen, G.: 2006, *J. Aerosol Sci.* **37**, 1683

Kocifaj, M., Klačka, J., Kundracík, F., Videen, G.: 2002, in *Optics of Cosmic Dust*, eds.: G. Videen and M. Kocifaj, Kluwer Academic Publishers, Dordrecht, Boston, London, 159

Kolokolova, L., Gustafson, B.Å.S.: 2001, *J. Quant. Spectrosc. Radiat. Transfer* **70**, 611

Lamy, Ph.L.: 1974, *å* **35**, 197

Levasseur-Regourd, A.Ch.: 2003, *Adv. Space Res.* **31**, 2599

Lumme, K., Rahola J.: 1998, *J. Quant. Spectrosc. Radiat. Transfer* **60**, 439

Mann, I., Kimura, H., Kolokolova, L.: 2004, *J. Quant. Spectrosc. Radiat. Transfer* **89**, 291

Maxwell Garnett, J.C.: 1904, *Philosphical Transactions of the Royal Society of London* **203**, 385

Mishchenko, M.I., Travis, L.D., Lacis, A.A.: 2002, *Scattering, Absorption, and Emission of Light by Small Particles*, Cambridge University Press, Cambridge

Moro-Martìn, A., Malhotra, R.: 2003, *Astron. J.* **125**, 2255

Mukai, T.: 1973, *Publ. Astron. Soc. Japan* **25**, 481
Mukai, T., Fechtig, H., Grün, E., Giese, R.H., Mukai, S.: 1986, *Astron. Astrophys.* **167**, 364
Muinonen, K.: 1996, *Earth, Moon, Planets* **72**, 339
Muinonen, K.: 2000, in *Light scattering by nonspherical particles*, eds.: M.I. Mishchenko, J.W. Hovenier and L.D. Travis, Academic Press, San Diego, San Francisco, New York, Boston, London, Sydney, Tokyo, 323
Notesco, G., Bar-Nun, A.: 2005, *Icarus* **175**, 546
Posch, T., Mutschke, H., Fabian, D.: 2002, *Hvar Obs. Bull.* **26**, 31
Purcell, E.M., Pennypacker, C.R.: 1973, *Astrophys. J.* **186**, 705
Quirantes, A., Delgado, A.V.: 2001, *J. Quant. Spectrosc. Radiat. Transfer* **70**, 261
Reach, W.T., Morris, P., Boulanger, F., Okumura, K.: 2003, *Icarus* **164**, 384
Schwehm, G.: 1976, in *Interplanetary dust and zodiacal light*, eds.: H. Elsässer and H. Fechtig, Springer-Verlag, Berlin, New York, 459
Le Sergeant D'Hendecourt, L.B., Lamy, Ph.L.: 1981, *Icarus* **47**, 270
Steel, D.I., Elford, W.G.: 1986, *Mon. Not. R. Astron. Soc.* **218**, 185
Sivasubramanian, S., Widom, A., Srivastava, Y.N.: 2005, *Physica A* **345**, 356
Sun, W., Nousiainen, T., Muinonen, K., Fu, Q., Loeb, N.G., Videen, G.: 2003, *J. Quant. Spectrosc. Radiat. Transfer* **79-80**, 1083
Swamy, K.S.K.: 1986, *Physics of comets*, World Scientific Publishing Co Pte Ltd, Singapore
Wickramasinghe, N.C.: 1967, *Interstellar grains*, Chapman and Hall Ltd, London
Williams, D.M., Mason, C.G., Gehrz, R.D., Jones, T.J., Woodward, C.E., Harker, D.E., Hanner, M.S., Wooden, D.H., Witteborn, F.C., Butner, H.M.: 1997, *Astrophys. J.* **489**, L91
Yeh, C.: 1964, *Phys. Rev. A* **135**, 1193
Zubko, E.S., Shkuratov, Y.G.: 2004, in *35th COSPAR Scientific Assembly*, ed.: M. Capria, COSPAR, Paris, 2454